RSC Advances

ROYAL SOCIETY
OF **CHEMISTRY**

www.rsc.org/advances

Journal Name RSCPublishing

ARTICLE

Size Dependence on the Polarization and Dielectric Properties of $KNbO_3$ Nanoparticles

Cite this: DOI: 10.1039/x0xx00000x

Haiyan Ge, Yuanye Huang, Yudong Hou, Han Xiao, and Mankang Zhu

Received 00th January 2012,
Accepted 00th January 2012

DOI: 10.1039/x0xx00000x

www.rsc.org/

Ferroelectric nanostructures have recently attracted much attention due to the continuous demand of miniaturizing devices and discovering novel phenomena. Therefore, depth study of the ferroelectric, and dielectric properties at various particle sizes in nanoscale ferroelectrics is of technological importance. Unfortunately, researches aimed at discovering and understanding size effect on electric properties of ferroelectric nanostructures are scarce. Here, we investigate the spontaneous polarization and dielectric constant at various sizes of nanocrystalline potassium niobates ($KNbO_3$) by using powder X-ray diffraction (XRD) Rietveld refinement, Raman spectroscopy, and the theoretical calculation. It is surprising to find that the spontaneous polarization P_s reaches at the highest value 40.3 μC/cm^2 at 100 nm, and decreases with increasing grain size from 100 nm to 500 nm. The dependence of dielectric constant on the grain size shows similar variation trend as that of spontaneous polarization. It is deduced that the large lattice distortion induced by lowering grain size facilitates the increase of P_s, which in turn contributes mainly to the enhancement of dielectric constant.

Introduction

Ferroelectric nanostructures, which intrinsically couple mechanical and electrical degrees of freedom, are attracting increasing attention.[1] These nanostructures are promising for nanoelectromechanical systems, with potential applications in the fields of nanosensors and actuators,[2, 3] energy harvesting,[4] and nanopiezotronics.[5] For the development of future nanodevices, ferroelectric nanoparticles should be handled and utilized. However, the biggest obstacle in the utilization of electric properties of nanosized ferroelectric particles is the "size effect". A large number of excellent researches have been performed on $PbTiO_3$,[6, 7] $PbZrO_3$,[8] and $BaTiO_3$,[9-11] which show the size effect on the crystal structure and phase transiton. Ishikawa and co-workers[6] intensively studied the $PbTiO_3$ fine particles by X-ray diffraction and Raman scattering. When the particle size is less than 50 nm, the transition temperature T_c decreases from its bulk value as the size decreases. For $BaTiO_3$ nanoparticles, many experimental studies have indicated that the phase-transition temperature is size-dependent, with the ferroelectric phase becoming unstable at room temperature when particle diameter decreases below a critical size. Wada *et al.*[9] found that the dielectric constant of $BaTiO_3$ particles with a size of around 70 nm exhibited a maximum of over 15000. Hoshina *et al.*[10] proposed a composite structure model including a gradient lattice strain layer (GLSL) between an inner tetragonal core and a surface cubic layer of $BaTiO_3$ particles to explain the size effect in $BaTiO_3$ nanoparticles. And Smith *et al.*[11] showed that the phase transition is diffuse in temperature for the smaller particles, in contrast to the sharp transition that is found for the bulk sample.

Recently, the electric polarization material of potassium niobates ($KNbO_3$, KN), regarded as an excellent lead-free piezoelectric and ferroelectric candidate, has been widely investigated.[12-14] Similar to $BaTiO_3$, $KNbO_3$ undergoes the same sequence of phase transitions, from a rhombohedral to an orthorhombic, a tetragonal and finally to a cubic as the temperature increases. However, the transition temperatures of $KNbO_3$ (263 K, 498 K and 708 K on heating) are considerably higher than those of $BaTiO_3$ (183 K, 278 K and 393 K).[15] Consequently, the room temperature structures of $KNbO_3$ and $BaTiO_3$ are respectively orthorhombic and tetragonal. It is reported that the single-crystal $KNbO_3$ can exhibit a large piezoelectricity and a high Curie point of 435°C.[16, 17] The electromechanical coupling factor of the thickness-extensional mode k_t, in a $KNbO_3$ crystal reaches as high as 0.69 for the 49.5° rotated *X*-cut about the *Y*-axis, which is the highest among current lead-free piezoelectrics.[18]

So, great interest has been generated for the study of size effects in $KNbO_3$ particles.[19-22] Chen et al.[19], in the study of $KNbO_3$ powders, obtained by the sol-gel method and having different particle sizes, from 40 to 80 nm, found that in this size range a change in the Curie temperature does not occur. However, Sawai *et al.*[20] has clarified that the presence of a critical size below 100 nm at which $KNbO_3$ transforms from orthorhombic to tetragonal phase at room temperature. At the same time, Golovina *et al.*[21] reported that the temperatures of all phase transitions of $KNbO_3$ nanostructure shift to a high-temperature region by 10 °C, 25 °C, and 40 °C compared with the relevant temperatures in bulk crystals and amount 0 °C, 248 °C, and 475 °C. It's implied that the manifestation of the size effect is especially significant with respect to the Curie temperature, i.e., for the ferroelectric phase transition. Finally, an unusual effect was observed by Louis *et al.*[22] in $KNbO_3$ nanowires, having an average diameter of 50 nm and a length of about 5 μm. It was found that the lowest-temperature phase in this material is not with rhombohedral but with monoclinic symmetry. On the other hand, the temperatures of all three transitions are the same as in macrocrystals. The works show a quite contradictory picture of the influence of particle size, both on the phase transition temperature and on the symmetry of nanoscale $KNbO_3$. However, due to the complexity of the phenomenon, the nature of particle size effect in piezoelectric $KNbO_3$ particles is still not well understood. To our limited knowledge in $KNbO_3$ particles, the effects of particle size on the electrical properties, such as ferroelectric and dielectric properties, have not yet been obtained. The main aim of this paper is to give experimental information about the problem.

In this work, we report on the successful preparation of reasonably pure, crystalline, single-phase $KNbO_3$ nanoparticles with controllable sizes (100, 200, 300, and 500 nm) through a large-scale, environmentally friendly molten salt synthesis method using a KCl salt, heated from 600 °C to 900 °C. It should be noted that the $KNbO_3$ nanoparticles with sizes below 100 nm could not be obtained in this case, because it is difficult to fabricate pure perovskite phase of $KNbO_3$ below 600 °C in molten salt synthesis process. We have studied the $KNbO_3$ nanoparticles by X-ray diffraction Rietveld refinements, Raman scattering, and the theoretical calculation. The spontaneous polarization and dielectric properties were investigated for the samples with various sizes. It is discovered that there exists a strong correlation among the spontaneous polarization, dielectric constant and particle size for $KNbO_3$ particles, which is important for the development of new generational nanodevices.

Experimental

In our experiment, the molten salt synthesis method was employed to prepare $KNbO_3$ nanoparticles with various sizes ranging from 100 to 500 nm. Analytical grade K_2CO_3 (99.0%), Nb_2O_5 (99.0%), and KCl (99.5%) were used as supplied. The choice of the molten salt medium KCl was governed by its relative non-toxicity, low melting temperature (770 °C) and not introducing impurity cations. In the typical synthesis of $KNbO_3$ nanoparticle, K_2CO_3, Nb_2O_5, and KCl were mixed in an overall stoichiometric ratio of 1 : 1 : 6 and ground for 24 h by ball milling in an ethanol medium. Before placing in an alumina crucible, the mixtures were pretreated at 120 °C for 6 h. The obtained dry mixtures were heated at a rapid rate of 8 °C /min up to 600 °C, 700 °C, 800 °C and 900 °C, respectively (abbreviated as KN1, KN2, KN3, and KN4) and maintained at that temperature for 4 h in air, and subsequently quenched to room temperature. Samples were immersed into deionized distilled water in a beaker to transfer the product into aqueous solution for subsequent separation and purification. The precipitates were centrifuged and purified with deionized distilled water several times, and dried in an oven at 120 °C for 8 h. We can easily and routinely scale up this molten salt synthesis process to produce grams of single-crystalline $KNbO_3$ nanoparticles.

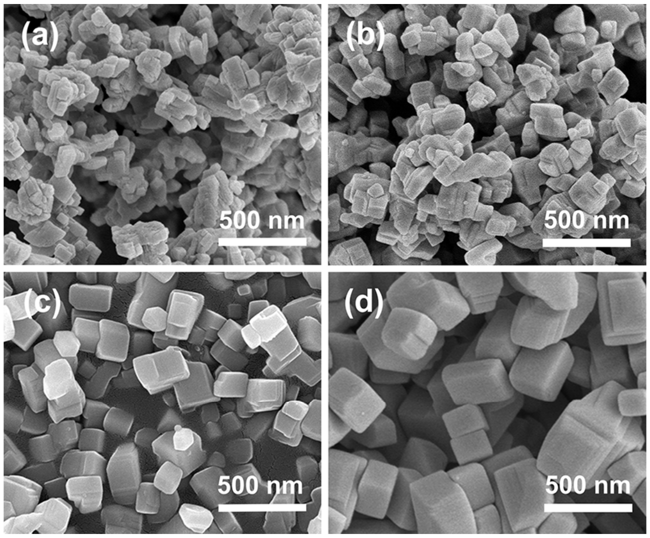

Fig. 1 Scanning electron micrographs of the as-prepared nanoparticles (a) KN1, (b) KN2, (c) KN3 and (d) KN4.

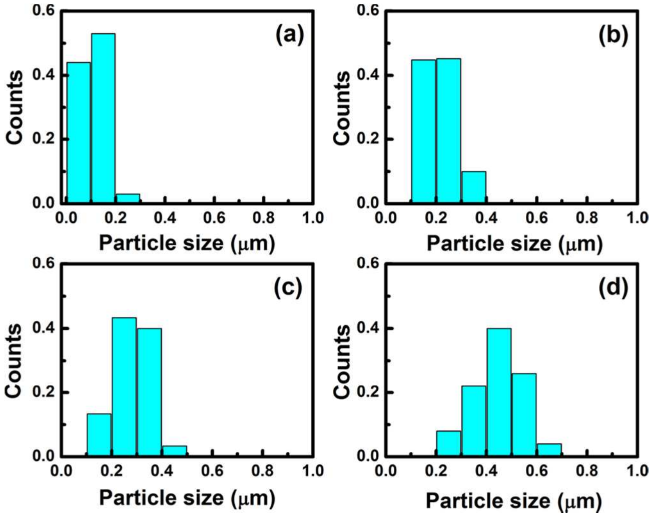

Fig. 2 Size distributions of the as-prepared nanoparticles (a) KN1, (b) KN2, (c) KN3 and (d) KN4.

For the measurements of dielectric properties, $KNbO_3$ nanoparticles with various sizes were used as the active phase and PVDF (Shanghai 3F Company, China) as the matrix with the high dielectric permittivity at room temperature. The PVDF was predispersed into an organic solution of N, N-dimethylformamide (DMF) prior to final mixing with the $KNbO_3$ nanoparticles. Then the slurry was ultrasonic dispersal for 30 min to form a transparent solution. The $KNbO_3$ nanoparticles were added into the transparent solution by means of ultrasonic dispersal for 10 min. Then the KN/PVDF mixture solution was stirred for 1 h. The mass fraction of the $KNbO_3$ nanoparticles was fixed at 50% of the total solid weight, which was used to ensure the connectivity of PVDF and at the same time to maximize the mass of $KNbO_3$. Finally, the mixture solution was dropped to a glass utensil and heated at 100 °C to evaporate the solvent completely. The resulting films were hot pressed for molding at 200 °C under a pressure of 200 MPa for 10 min. The final samples of disk shape were 15 mm in diameter and about 1 mm in thickness. For electrical measurements, the upper and lower surfaces of the disks were coated with silver paste.

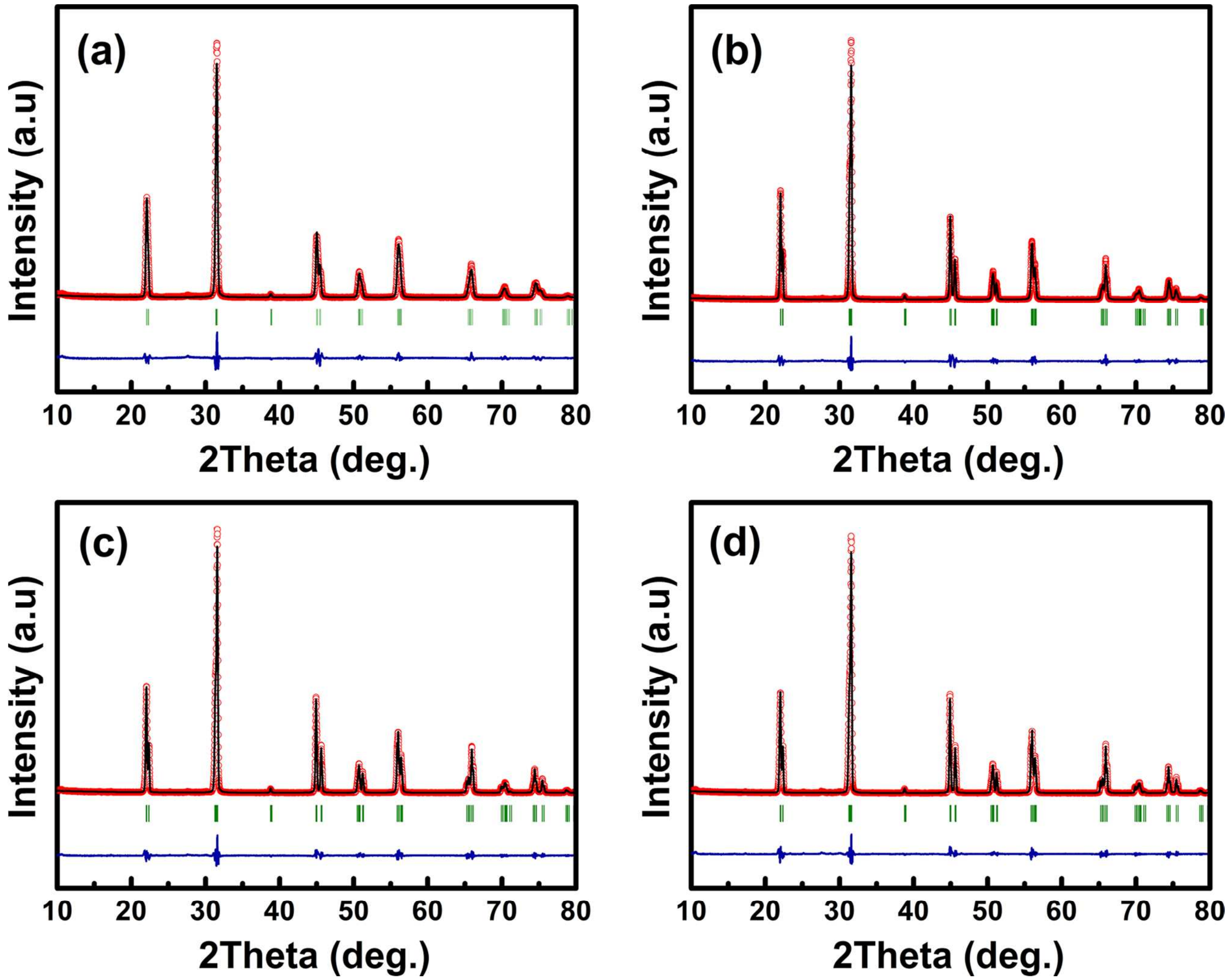

Fig. 3 Observed (circles), calculated (line), and differential (bottom of figure) X-ray powder diffraction profiles for (a) KN1, (b) KN2, (c) KN3 and (d) KN4 obtained after the Rietveld refinements at room temperature. The tick marks give the positions of all possible Bragg reflections.

Powder X-ray diffraction (XRD) data were collected by using an automated diffractometer (Bruker D8 Advance, Karlsruhe, Germany) with Cu Kα radiation ($\lambda = 1.541$ Å) at room temperature. The patterns were collected over an angular range of 10 - 80° with a step width of 0.01 degrees and a 2.5 s per step counting rate. The microstructural features were observed by scanning electron microscopy (SEM, Hitachi S-3500). Raman spectra were recorded in the frequency range 100-1000 cm^{-1} on a Raman spectrometer (Spex 1403, American) with a solid-state laser (excitation at 488 nm) at room temperature. The laser power was kept low enough to avoid heating of the samples by optical filtering and defocusing the laser beam at the sample surface. The dielectric constant ε_r and loss tangent tan δ were measured in the frequency range from 10^2 to 10^7 at room temperature using an automated dielectric measurement system with a inductance capacitance resistance (LCR) meter (Agilent E4294A, Santa Clara, CA).

Results and discussion

To reveal the morphology and size dispersion of the particles, the $KNbO_3$ powders were examined using the scanning electron microscopy (SEM). Fig. 1 shows the SEM images of all four $KNbO_3$ nanoparticles. It is evident that the products mainly consist of solid, crystalline particles, although the particle morphology is dependent on the crystal structure of the material.

Table 1 Crystallographic Data and Structure Refinement Parameters of all four $KNbO_3$ nanoparticles by X-Ray Powder Diffraction

		KN1	**KN2**	**KN3**	**KN4**
Crystal system		orthorhombic	orthorhombic	orthorhombic	orthorhombic
Space group		*Amm*2	*Amm*2	*Amm*2	*Amm*2
Lattice parameters	a(Å)	3.98913(12)	3.97834(07)	3.97487 (06)	3.97493 (06)
	b(Å)	5.68736(30)	5.69266(12)	5.69302 (09)	5.69354 (09)
	c(Å)	5.69674(28)	5.70769(11)	5.71263 (09)	5.71556 (09)
Cell volume	V(Å^3)	129.245(10)	129.264(04)	129.271(03)	129.351(03)
Agreement factors	R_{wp}(%)	12.7	11.5	10.2	10.5
	R_p(%)	8.94	7.85	6.89	6.88
	R_{exp}(%)	5.79	5.48	5.3	5.19
	χ^2	4.81	4.40	3.70	4.09

Table 2 Atoms displacements (Å) of all four $KNbO_3$ nanoparticles by X-Ray Powder Diffraction

	KN1	**KN2**	**KN3**	**KN4**
Δz(K)	0.00918(369)	0.01127(221)	0.01444(166)	0.01646(155)
$\Delta z(O_I)$	0.06330(323)	0.05284(285)	0.03943(240)	0.03895(235)
$\Delta z(O_{II})$	0.01664(475)	0.02325(272)	0.02868(196)	0.02604(200)
$\Delta y(O_{II})$	0.00641(585)	0.00538(331)	0.00312(237)	0.00289(288)

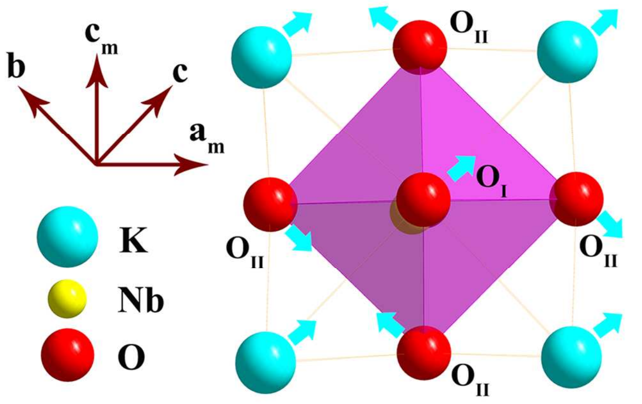

Fig. 4 The monoclinic subcell is projected along orthorhombic *a*-axis (the *b* and *c* corresponding orthorhombic axes), and the arrows indicate the displacement direction.

In particular, the $KNbO_3$ particles sample annealed at 900 °C is composed of solely submicron-scale cubes, which have distinct edges. With decreasing the annealing temperature, the sharp, distinct edges of the initial cube smoothen, eventually changed to agglomerate nanostructures. As-prepared $KNbO_3$ particle samples are free of hard agglomeration, although it is apparent that there is some degree of loose aggregation in these nanostructures, accounting for the clumping observed in the SEM images. SEM images have been taken from randomly selected areas of the substrate, and as such, these are representative of the overall sizes and shapes of $KNbO_3$ particles in the samples. Using Image Pro Plus software, the distributions of particle sizes have been further analysed and the results are present in Fig 2. It is showed that the median particle sizes of $KNbO_3$ nanoparticles (KN1, KN2, KN3 and KN4) are about 100, 200, 300, and 500 nm, respectively. The particle size grows gradually as the calcining temperature increases, which could be attributed to accelerated crystal growth in high temperature molten salt media. This phenomenon was also observed for the cuboidal $LaAlO_3$ in molten salt synthesis process.[23]

In order to characterize structures of the prepared oxides, XRD Rietveld refinements for the KN1, KN2, KN3 and KN4 were carried out with *Amm*2 space group at room temperature, by using the FULLPROF software.[24] During the refinement process, Nb atom was fixed at the origin (0,0,0). The peak profiles were fitted with the Pseudo-Voigt function. In addition to the occupation numbers of atoms, which were fixed at the nominal composition, all other parameters, such as scale factor, zero correction, background, half-width parameters, lattice parameters, positional coordinates, and thermal parameters, were varied in the process of structure refinement. It was necessary to employ the mode of anisotropic peak broadening for the full-profile fitting of XRD data. As shown in Fig. 3(a)-(d), the calculated diffraction profiles agree well with the observed ones for the KN1, KN2, KN3 and KN4, respectively. The detail Crystallographic Data and Structure Refinement Parameters are summarized in Table 1.

Although the structure of $KNbO_3$ at room temperature is orthorhombic, the perovskite type ABO_3 subcell possesses monoclinic symmetry, with lattice parameters $a_m = c_m > b_m$ while b_m-axis is perpendicular to $a_m c_m$ plane and angle β a little more than 90°.[25] According to the refined structural parameters, the projection of monoclinic subcell along orthorhombic a-axis (b_m-axis) was shown in Fig. 4, and the arrows indicated the displacement direction. With respect to Nb at origin, the K atoms and O_I atoms displace from its original position along the positive c direction. The O_{II} atoms shift in the same direction. In addition, the O_{II} atoms have larger displacements in the c direction than the b direction. Therefore, the spontaneous polarization directions of orthorhombic $KNbO_3$ correspond to $[101]_m$ (c-axis). The atoms displacements are calculated and listed in Table 2. It can be obviously found that, the variation of O_I displacements is smaller than that of K atoms and O_{II} with increasing grain size. The displacement of K atoms along the z-axis and that of O_{II} along the z-axis sharply increas, while that of O_{II} along the y-axis rapidly decreases. Therefore, O_{II}'s contribution to the spontaneous polarization along the $[101]_m$ sharply decrease while K atoms contribution to the spontaneous polarization increases.

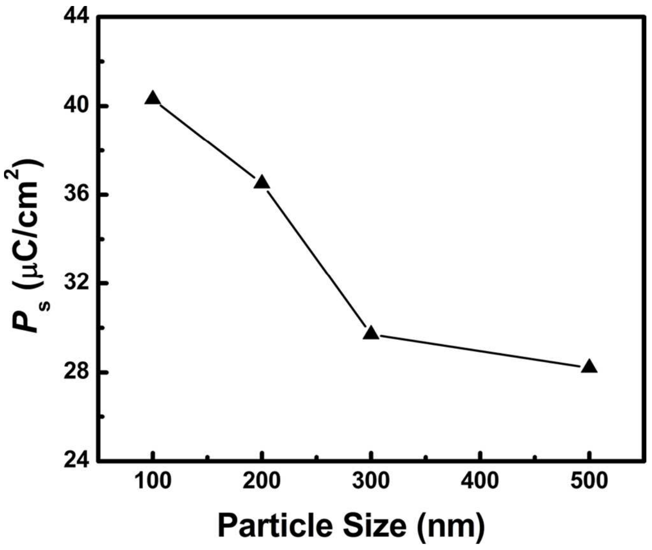

Fig. 5 Variation of the spontaneous polarization (P_s) as a function of particle size of $KNbO_3$.

It is well known that the atom displacement is directly related to the ferroelectric characters of this perovskite-type structure. So, the spontaneous polarization (P_s) due to the relative ion displacements can be basically estimated by considering a purely ionic crystal and neglecting the electronic polarization

$$P_s = \frac{e}{V}\sum_i z_i'' \Delta i \tag{1}$$

where V is the unit cell volume, Δi is the shifts of the ith atom along the ferroelectric axis, z_i'' is the apparent charge.[26] In terms of the atoms displacements in Table 2, the spontaneous polarization (P_s) as a function of grain size of $KNbO_3$ are calculated and shown in Fig. 5. These calculated values can be considered as an upper limit of the P_s for the experimental measurement. Apparently, the calculated spontaneous polarization (P_s) increases with decreasing grain size from 500nm to 100nm, and the maximum P_s value (40.3 μC/cm^2) is obtained at about 100nm. It implies that the spontaneous polarization (P_s) was strongly influenced by the grain size.

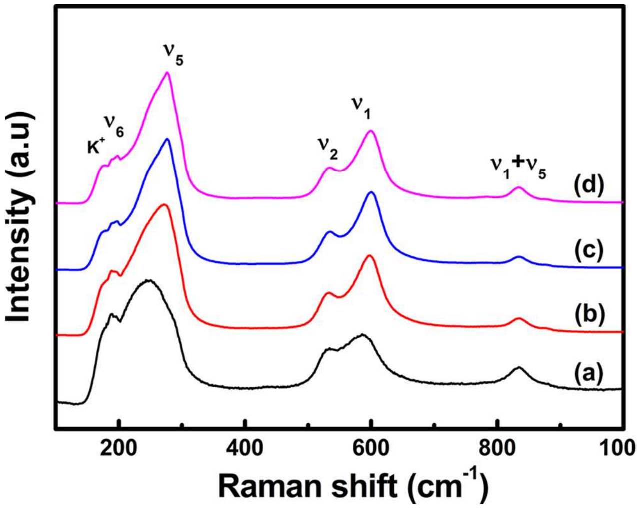

Fig. 6. Raman spectra of the as-prepared samples for (a) KN1, (b) KN2, (c) KN3 and (d) KN4 at room temperature.

Raman spectra are known to be an appropriate technique for the investigation of the short-range order and phase structure in perovskites. To further affirm the lattice distortion as a function of annealing temperature, all four samples were examined by Raman scattering. For $KNbO_3$ single crystal, there are three obvious ranges appearing, in an ascending order, at around 280, 597, and 836 cm^{-1} in the Raman shift range of 100 - 1000 cm^{-1} in the early reported data.[27] Fig. 6 shows Raman spectra of $KNbO_3$ nanostructure obtained at the different annealed temperature from 600 °C to 900 °C in the frequency range of 100 - 1000 cm^{-1}. It can be clearly seen that the first range at 246 cm^{-1} shifts upward to 281 cm^{-1} when the annealed temperature change from 600 °C to 900 °C. The annealed temperature may induce the distortion and shrinkage of the lattice parameters, which results in the enhancement of both the force constant $[BO_6]$ in the lattice and the stability of the centered ion in the oxygen octahedron. This effect may cause the range to shift to higher wave numbers. On the other hand, as the temperature increases, the intensity difference of the bands at between 528 cm^{-1} and 586 cm^{-1} begins to augment, which gives another evidence of the lattice distortion.[28]

In order to investigate the dielectric properties of pure perovskite structure $KNbO_3$ nanocrystals, four $KNbO_3$ samples were selected as the active phase dispersed into the matrix PVDF, and then were molded by hot-pressing at 200 °C. To image the morphology of the composites after melt processing, the cross-sections of a typical KN/PVDF composite with KN1, KN2, KN3 and KN4 nanoparticles were characterized by SEM. As shown in Fig. 7, the polymer is self-connected into a continuous network, which plays the role of binder, and the $KNbO_3$ nanoparticles are uniformly dispersed in the polymer although there is a small quantity of $KNbO_3$ aggregation in Fig. 7(a). There are few air voids or defects in the KN/PVDF composites. It is evidenced that the KN/PVDF composites prepared by this two-step mixing method and hot-press processing show very compact structure. This densified structure is in favour of characterising the electrical properties of the KN/PVDF composites.

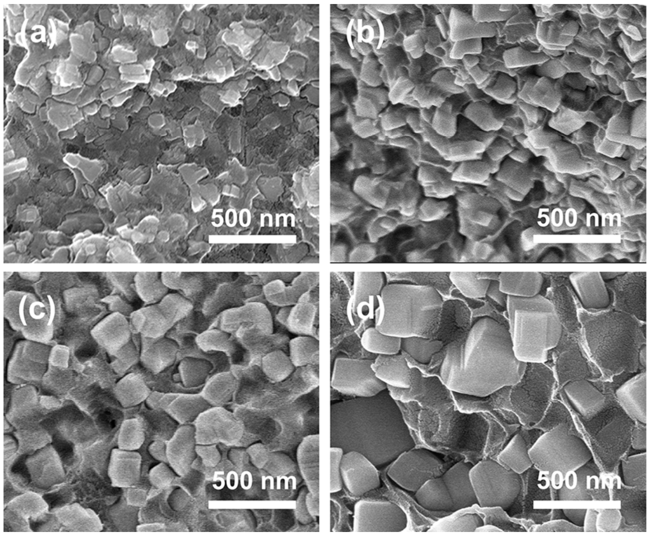

Fig. 7 Scanning electron micrographs of the cross-section for the typical KN/PVDF composites with (a) KN1, (b) KN2, (c) KN3 and (d) KN4.

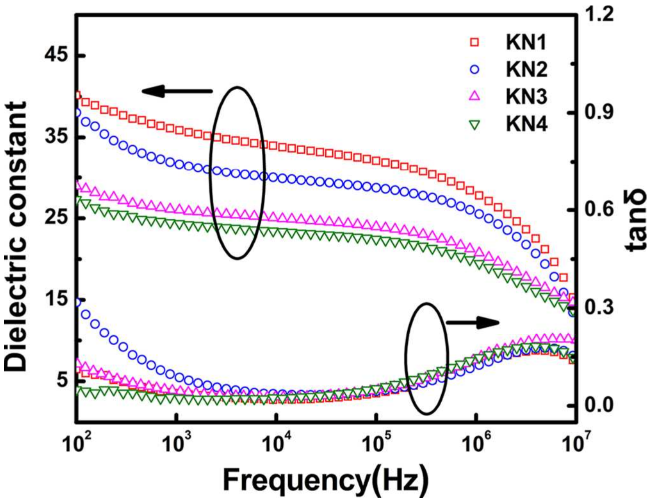

Fig. 8 The frequency dependences of the dielectric constant ε_r and loss tangent tan δ at room temperature for the $KNbO_3$/PVDF composite with various particle sizes.

The frequency dependences of the dielectric constant ε_r and loss tangent tan δ at room temperature were measured for the KN/PVDF composites with $KNbO_3$ particles of four sizes (Fig. 8). All the KN/PVDF composites have a relatively low dielectric loss (less than 0.15), which may arise from low particle-polymer interfacial energy and small relaxing polarization current in the composites. Within the frequency range from 10^2 Hz to 10^6 Hz, there is one of the advantages of this kind of composite: the weak dependence of its dielectric constant on the frequency. In addition, an obvious difference in the dielectric constant between KN/PVDF composite with four sizes could be observed. The dielectric constant of KN4/PVDF composite was lowest, the dielectric constant of KN3/PVDF composite was lower than that of KN2/PVDF composite, and the dielectric constant of KN1/PVDF composite was the highest. This result may be attributed to the dielectric constant difference of inorganic particles themselves.

The dependence of the room temperature dielectric constant (at 100Hz) of the KN/PVDF composites on the $KNbO_3$ nanoparticle size is shown in Fig. 9(a). The dielectric constant exhibits a minimum (ε_r = 27.29) and a maximum (ε_r = 40.15) value at the $KNbO_3$ particle size of 500 nm and 100 nm, respectively. In order to acquire the dielectric constant of the $KNbO_3$ nanoparticles from the KN/PVDF composites, the theoretical calculated modes was employ. Mixing laws approaches are used most commonly for predicting the dielectric constant of a continuous polymer matrix filled with uniformly distributed inorganic particles.[29] According to the Modified Rother-Lichtenecker equation,[30] the measured dielectric constant ($\varepsilon_{measured}$) is given by the relation

$$\varepsilon_{measured} = \exp[\ln\varepsilon_1 + f_2(1-k)\ln(\varepsilon_2/\varepsilon_1)] \qquad (2)$$

where $\varepsilon_{measured}$, ε_1, and ε_2 stand for the dielectric constant of the KN/PVDF composite, the PVDF (the matrix phase), and the $KNbO_3$ nanoparticle (the active phase), respectively, f_2 represents the volume fraction of the $KNbO_3$ nanoparticle, and k is the shape dependent parameter (k = 0.5). Note that the equation is applicable for non-percolating, well-dispersed particles. Fig. 9(b) shows the corresponding dielectric constant of the $KNbO_3$ nanoparticles at various particle sizes. The dielectric constant of 100 nm-sized $KNbO_3$ particles exhibits the maximum value of 2599, which is potential in application as dielectric nano-device. However, with the increase of particle size, the dielectric constant exhibits the decreasing trend. The dielectric constant of 500 nm-sized $KNbO_3$ particle is only 554, which is slightly larger than that reported in bulk $KNbO_3$ ceramics with the grain size about 4 μm (ε_r = 528[31, 32]). Namely, the calculation results from the Modified Rother-Lichtenecker equation was in good agreement with the experimental data and this equation could be used to calculate the effective dielectric constant of $KNbO_3$ nanoparticles undoubtedly. Based on the former observation in the spontaneous polarization (P_s) of the $KNbO_3$ nanoparticles, it can be clearly found that the variation tendency of the dielectric constant at various particle sizes was consistent with that of P_s. This phenomenon is not strange as that for ferroelectric materials, spontaneous polarization is the primary form of polarization, which contributes mainly to the dielectric constant. However, during the sizes scales in our study, the critical size for phase transformation from orthorhombic to tetragonal phase does not occur. For the well accepted wisdom that niobates get super piezoelectric properties in orthorhombic to tetragonal transition region, the preparation and study of low sized (below 100nm) particles are most needed, and though difficult, these works are now under the way.

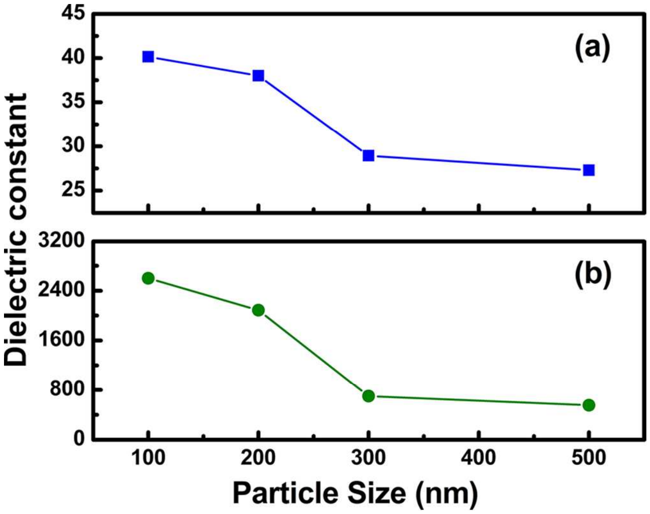

Fig. 9 Size-dependence of the dielectric constants for (a) the $KNbO_3$/PVDF composites measured at room temperature, (b) the $KNbO_3$ nanoparticles calculated using theoretical model.

Conclusions

The size effect on polarization and dielectric properties was key issues to develop nanoelectromechanical transducers in the future. So, we investigate the spontaneous polarization and dielectric constant at various sizes of nanoparticles $KNbO_3$ by using powder X-ray diffraction (XRD) Rietveld refinement, Raman spectroscopy, and the theoretical calculation. Our research shows that the spontaneous polarization P_s is increase with decreasing particle size from 500 to 100 nm, and reaches at the highest value 40.3 $\mu C/cm^2$ at 100 nm. Due to the contribution from the enhanced spontaneous polarization, 100 nm sized $KNbO_3$ particle present the maximum value of dielectric constant (2599), which is potential in application as dielectric nano-device. The present work is better understanding for size effect on ferroelectric and dielectric properties in $KNbO_3$ nanoparticles and useful to study other ferroelectric nanoscale materials.

Acknowledgements

The work is partially supported by the National Natural Science Foundation of China (Grant No. 51072008, No.51172006), the Natural Science Foundation of Beijing (Grant No.2132007), Specialized Research Fund for the Doctoral Program of Higher Education of China (No.20131103110031) and the Foundation on the Creative Research Team Construction Promotion Project of Beijing Municipal Institutions.

Notes and references

College of Materials Science and Engineering, Beijing University of Technology, Beijing 100124, China. E-mail: ydhou@bjut.edu.cn; Fax: +86-10-67392445; Tel: +86-10-67392445

1 Z. L. Wang and J. H. Song, *Science*, 2006, **312**, 242-246.
2 X. Wang, J. Zhou, J. Song, J. Liu, N. Xu and Z. L. Wang, *Nano Lett*, 2006, **6**, 2768-2772.
3 C. S. Lao, Q. Kuang, Z. L. Wang, M.-C. Park and Y. Deng, *Appl. Phys. Lett.*, 2007, **90**, 262107.
4 X. D. Wang, J. H. Song, J. Liu and Z. L. Wang, *Science*, 2007, **316**, 102-105.
5 P. X. Gao, J. H. Song, J. Liu and Z. L. Wang, *Adv. Mater.*, 2007, **19**, 67-72.
6 K. Ishikawa, K. Yoshikawa and N. Okada, *Phys. Rev. B*, 1988, **37**, 5852-5855.
7 K. Ishikawa, T. Nomura, N. Okada and K. Takada, *Jpn. J. Appl. Phys.*, **35**, 5196-5198.
8 C. Soma, A. Pushan, V. R. Palkar, A. V. Gurjar, R. M. Wankar and M. Manu, *Journal of Physics: Condensed Matter*, 1997, **9**, 8135.
9 S. Wada, H. Yasuno, T. Hoshina, S. M. Nam, H. Kakemoto and T. Tsurumi, *Jpn. J. Appl. Phys.*, 2003, **42**, 6188-6195.
10 T. Hoshina, S. Wada, Y. Kuroiwa and T. Tsurumi, *Appl. Phys. Lett.*, 2008, **93**, 192914.
11 M. B. Smith, K. Page, T. Siegrist, P. L. Redmond, E. C. Walter, R. Seshadri, L. E. Brus and M. L. Steigerwald, *J. Am. Chem. Soc.*, 2008, **130**, 6955-6963.
12 T. V. Murzina, S. A. Savinov, A. A. Ezhov, O. A. Aktsipetrov, I. E. Korsakov, I. A. Bolshakov and A. R. Kaul, *Appl. Phys. Lett.*, 2006, **89**, 062907.
13 L. H. Li, J. X. Deng, J. Chen, X. Y. Sun, R. B. Yu, G. R. Liu and X. R. Xing, *Chem. Mater.*, 2009, **21**, 1207-1213.
14 S. Kim, J. H. Lee, J. Lee, S. W. Kim, M. H. Kim, S. Park, H. Chung, Y. I. Kim and W. Kim, *J. Am. Chem. Soc.*, 2013, **135**, 6-9.
15 G. Shirane, R. Newnham and R. Pepinsky, *Phys. Rev.*, 1954, **96**, 581-588.
16 S. Wada, A. Seike and T. Tsurumi, *Jpn. J. Appl. Phys.*, 2001, **40**, 5690-5697.
17 K. Nakamura, T. Tokiwa and Y. Kawamura, *J. Appl. Phys.*, 2002, **91**, 9272-9276.
18 K. Nakamura and Y. Kawamura, *IEEE Trans. Ultrason. Ferroelectr. Freq. Control*, 2000, **47**, 750-755.
19 H. Y. Chen, Y. X. Zhang and Y. L. Lu, *Nanoscale Res. Lett.*, 2011, **6**.
20 S. Sawai, H. Yamada, A. Iba, H. Tanaka, Y. Matsumoto and K. Tomita, *Ferroelectrics*, 2012, **433**, 45-52.
21 I. S. Golovina, V. P. Bryksa, V. V. Strelchuk, I. N. Geifman and A. A. Andriiko, *J. Appl. Phys.*, 2013, **113**.
22 L. Louis, P. Gemeiner, I. Ponomareva, L. Bellaiche, G. Geneste, W. Ma, N. Setter and B. Dkhil, *Nano Lett*, 2010, **10**, 1177-1183.
23 Z. S. Li, S. W. Zhang and W. E. Lee, *J. Eur. Ceram. Soc.*, 2007, **27**, 3201-3205.

24 T. Roisnel and J. Rodriguez-Carvajal, *Materials Science Forum*, 2001, **378-381**, 118-123.
25 V. J. Tennery and K. W. Hang, *J. Appl. Phys.*, 1968, **39**, 4749-4753.
26 A. W. Hewat, *Journal of Physics C: Solid State Physics*, 1973, **6**, 2559-2572.
27 Z. X. Shen, Z. P. Hu, T. C. Chong, C. Y. Beh, S. H. Tang and M. H. Kuok, *Phys. Rev. B*, 1995, **52**, 3976-3980.
28 Y. F. Chang, Z. P. Yang, Y. T. Hou, Z. H. Liu and Z. L. Wang, *Appl. Phys. Lett.*, 2007, **90**, 232905.
29 G. Subodh, C. Pavithran, P. Mohanan and M. T. Sebastian, *J. Eur. Ceram. Soc.*, 2007, **27**, 3039-3044.
30 Z. Ahmad, A. Prasad and K. Prasad, *Physica B*, 2009, **404**, 3637-3644.
31 H. Y. Ge, Y. D. Hou, M. K. Zhu, H. Wang and H. Yan, *Chem. Commun.*, 2008, **41**, 5137-5139.
32 H. Y. Ge, Y. D. Hou, C. Wang, M. K. Zhu and H. Yan, *Jpn. J. Appl. Phys.*, 2009, **48**, 041405.

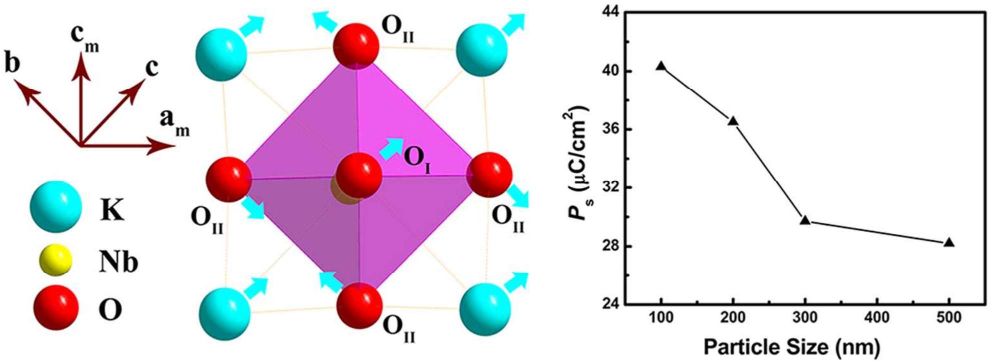

The spontaneous polarization and dielectric constant of nanocrystalline KNbO3 were strongly influenced by the particle size, and reached at the highest value at 100 nm. The present work is useful to study other ferroelectric nanoscale materials.
99x36mm (300 x 300 DPI)